

Article

Homo-Polymerization of 1-Hexene Catalysed by O[^]N[^]N (Salicylaldimine)Iron(III) Pre-Catalysts to Branched Poly(1-hexene)

Margaret Yankey, Collins Obuah and James Darkwa *

Department of Chemistry, University of Johannesburg, Auckland Park Kingsway Campus, Auckland Park, 2006, South Africa; margaretyankey@gmail.com (M.Y.); cobuah@yahoo.co.uk (C.O.)

* Correspondence: jdarkwa@uj.ac.za; Tel.: +27-11-559-2838

Academic Editor: Carl Redshaw

Received: 22 September 2015; Accepted: 2 March 2016; Published: 17 March 2016

Abstract: Five new iron(III) 1-hexene polymerisation catalysts were prepared from the reactions of 2,4-di-*tert*-butyl-6-(2-(1H-imidazol-4-yl)ethylimino)methylphenol (**L1**), or 4-*tert*-butyl-6-(2-(1H-imidazol-4-yl)ethylimino)methylphenol (**L2**) or 2,4-di-*tert*-butyl-6-[(2-pyridin-2-yl-ethylimino)-methyl-phenol (**L3**) with anhydrous iron(II) halides to form [FeCl₂(**L1**)] (**1**), [FeBr₂(**L1**)] (**2**), [FeI₂(**L1**)] (**3**), [FeBr₂(**L2**)] (**4**) and [FeCl₂(**L3**)] (**5**). All the iron(III) complexes **1–5** were activated with EtAlCl₂ to produce active catalysts for the polymerisation of 1-hexene to low molecular weight poly(1-hexene) ($M_n = 1021–1084$ Da) and very narrow polydispersity indices (1.19–1.24). ¹H and ¹³C{¹H} NMR analysis showed the polymers are branched with methyl, butyl and longer chain branches. The longer chain branches are dominant indicating that 2,1-insertion of monomer is favoured over 1,2-insertion in the polymerisation reaction.

Keywords: (salicylaldimine)iron(III) pre-catalysts; 1-hexene polymerisation; branched low molecular weight poly(1-hexene); narrow polydispersity indices

1. Introduction

The polymerisation of α -olefins to low molecular weight, hyper-branched polymers with narrow molecular weight distribution is of considerable interest. These hyper-branched polymers have applications as lubricants and as starting materials for lubricant additives [1]. The production of these low molecular weight hyper-branched polymers has been catalysed mainly by metallocenes [2–7]. The metallocene catalysts provide access to new or improved materials but at a high cost. The metallocene catalysts are also quite sensitive to either moisture or air and in some instances even to both moisture and air. As such there is great interest in finding late transition metal catalysts that have lower cost and are stable to both moisture and air for the polymerisation of α -olefins [8–16]. Such late transition metal catalysts should have other desirable properties such as being less oxophilic and hence tolerant toward functional groups [11,12,15,16]. Furthermore the late transition metal catalysts should be able to undergo “chain-walking” reactions [9,10,14–18] thereby producing a variety of novel branched olefin polymers.

Brookhart and co-workers [11,17,19–22] and others [23–25] have investigated extensively the polymerisation of ethylene with nickel(II) and palladium(II) catalysts. The type of polyethylenes produced by these nickel and palladium catalysts range from highly branched, amorphous materials to semi crystalline high density materials. Higher α -olefins, such as propylene and 1-hexene, have also been polymerised into amorphous or atactic polymers with these catalysts [17]. Through variations in the ligand design, reaction conditions and type of monomer used, novel elastomeric multiblock poly(α -olefin) [19–22] and regioblock co-polymers [26–28] have been

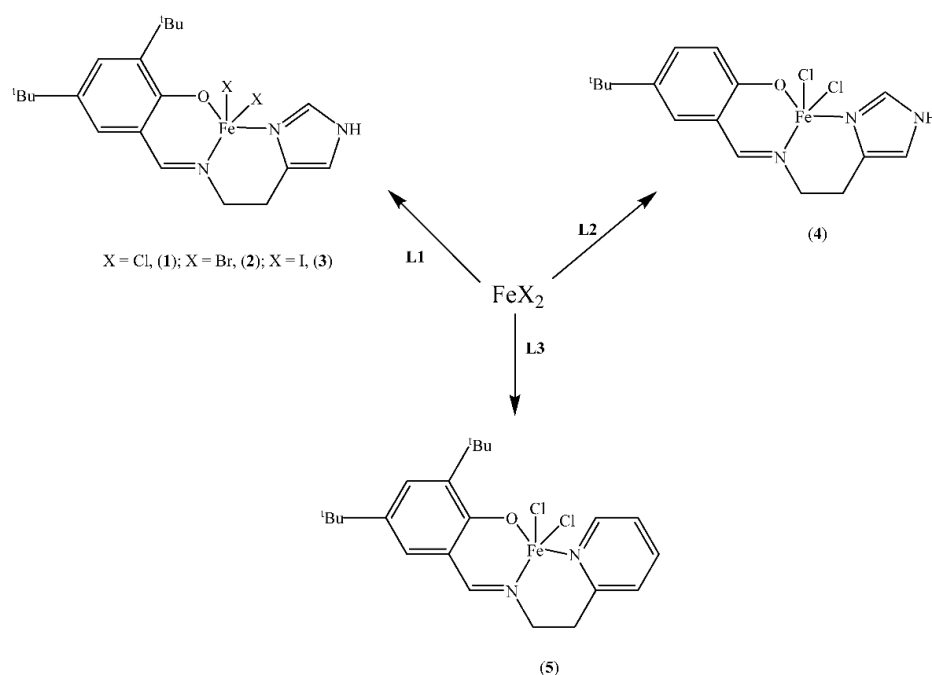
synthesised. In particular, cationic nickel(II) catalysts have been found to produce polyethylene, polypropylene and poly(1-hexene) [29–33] that have significant branching. Iron(II) and cobalt(II) catalysts, bearing bis(arylimino)pyridine ligands, have also been studied for the polymerisation of ethylene [34–36]. These iron and cobalt catalysts produce medium to high molecular weight polyethylenes that depend on the ligand structure of the catalyst [37–41]; thus, ligand modifications does not only affect the productivity of the catalysts but also the molecular weight and the microstructure of the polyolefin formed [37,38,40,41]. For example isospecific polymerization of propylene with iron(II) catalysts produce isotactic materials with activities exceeding $1600 \text{ kg}_{\text{polymer}} \text{ mol}_{\text{Fe}}^{-1} \text{ h}^{-1}$ [42]. There, however, have been limited studies on iron catalysed higher α -olefins polymerisation. One example of iron catalysed polymerisation of higher α -olefins is the head to head dimerization of 1-hexene reported by Small *et al.* [43]. As such our report is the first example of 1-hexene reaction that goes beyond dimerization.

We report on the polymerisation of 1-hexene with various (salicylaldimine)iron(III) halide pre-catalysts. ^1H and $^{13}\text{C}\{^1\text{H}\}$ NMR spectroscopy of the poly(1-hexene) produced in this study show branched microstructures. Details of this study are provided in this report.

2. Results and Discussions

2.1. Syntheses of (Salicylaldimine)Iron(III) Complexes

The syntheses of the O NN -(salicylaldimine)iron(III) complexes **1–4** (Scheme 1) have been reported by us recently [44]; but complex **5** (Scheme 1) is new and was synthesised following a similar procedure in the literature [44]. The reaction of iron(II) chloride with 2,4-di-*tert*-butyl-6-[(2-pyridin-2-yl-ethylimino)-methyl]-phenol (**L3**) formed the iron(III) complex $[\text{FeCl}_2(\text{L3})]$. Similar to the syntheses of **1–4** [44], we envisage that the intermediate iron(II) complex $[\text{FeCl}(\text{L3})]$ was formed, which is then oxidized by HCl (a by-product from the reaction) to the iron(III) product $[\text{FeCl}_2(\text{L3})]$ (**5**). Micro analysis and high resolution mass spectral data were in agreement with the proposed structure of complex **5** in Scheme 1, which suggested that the coordination of **L3** in **5** is through the phenoxy-O, the imine-N and the pyridine-N similar to the single crystal X-ray structures of complexes **1** and **2** [44].



Scheme 1. O NN -(salicylaldimine)iron(III) pre-catalysts as catalysts for polymerisation of 1-hexene.

2.2. Polymerisation of 1-hexene

The ability of all the (salicylaldimine)iron(III) complexes **1–5** to polymerise 1-hexene was investigated by activating the complexes with EtAlCl₂ at an optimum Al:Fe ratio of 400:1. The polymerisation reactions were performed in hexane at varying reaction temperatures from 30–60 °C. When GC analysis showed no evidence of 1-hexene oligomers, the reaction mixtures were worked up by evaporating the solvent to give viscous oily products. Catalysts activities ranged from 2.17×10^6 to 2.83×10^6 g_{polymer} mol_{Fe}⁻¹ h⁻¹ (Table 1: entries 1–5). GPC data for these products showed them to be low molecular weight poly(1-hexenes) that have *M_n* values slightly higher than 1000 Da. The polydispersity indices of the poly(1-hexene) produced by all the catalysts are relatively narrow (1.19–1.24) (Table 1), indicative of the single-site nature of the (salicylaldimine)iron(III) catalysts. Changing the second N-donor in the ligand from imidazolyl (2.83×10^6 g_{polymer} mol_{Fe}⁻¹ h⁻¹, Table 1: entry 1) to pyridyl (2.31×10^6 g_{polymer} mol_{Fe}⁻¹ h⁻¹, Table 1: entry 5) resulted in a decrease in catalyst activity; an observation that can be attributed to the weaker σ-donor ability of the imidazolyl group in pre-catalyst **1** compared to the pyridyl group in pre-catalyst **5**, which makes the iron centre in the (imidazolylsalicylaldimine)iron(III) catalyst (**1**) more electrophilic and hence more active than the (pyridylsalicylaldimine)iron(III) catalyst (**5**). Complex **4** is the least active most likely because of its low solubility. The activity of the chloro iron(III) pre-catalyst **1** (2.83×10^6 g_{polymer} mol_{Fe}⁻¹ h⁻¹) was found to be slightly higher than the bromo iron(III) catalyst **2** (2.35×10^6 g_{polymer} mol_{Fe}⁻¹ h⁻¹) and the iodo iron(III) catalyst **3** (2.25×10^6 g_{polymer} mol_{Fe}⁻¹ h⁻¹). This can be attributed to the chloride ion being a stronger conjugate base than the bromide and iodide ions, and hence is readily abstracted by the EtAlCl₂ co-catalyst. All three catalysts nevertheless produced poly(1-hexene) with identical properties (Table 1: entries 1–3).

Table 1. Polymerisation of 1-hexene using salicylaldimine-iron(III) pre-catalysts **1–5** and EtAlCl₂ as cocatalyst ^a.

Entry	Pre-Catalyst	Temperature (°C)	Yield (g)	Activity ^b × 10 ⁶	<i>M_n</i> ^c (Da)	<i>M_w</i> ^c (Da)	<i>M_w</i> / <i>M_n</i> ^c
1	1	30	0.68	2.83	1045	1273	1.22
2	2	30	0.57	2.35	1059	1296	1.22
3	3	30	0.54	2.25	1068	1318	1.23
4	4	30	0.53	2.17	1079	1342	1.24
5	5	30	0.56	2.31	1063	1312	1.23
6	1	40	0.69	2.88	1037	1263	1.22
7	1	50	0.74	3.10	1029	1253	1.22
8	1	60	0.58	2.42	1021	1240	1.21
9 ^d	1	30	0.64	2.67	1038	1237	1.19
10 ^e	1	30	0.66	2.77	1084	1339	1.24

^(a) Reaction conditions: Hexane (10 mL), Fe (11 μmol), Al:Fe (400:1), monomer equivalent (2000);

^(b) Activity = g_{polymer} mol_{Fe}⁻¹ h⁻¹; ^(c) Determined by GPC using polystyrene standards; ^(d) monomer equivalent (1500); ^(e) monomer equivalent (2500).

The effects of reaction temperature and monomer equivalents were investigated using **1**/EtAlCl₂. The effect of reaction temperature on the polymerisation activity of **1**/EtAlCl₂ was conducted over 60 min at Al:Fe ratio of 400:1 (Table 1: entries 1 and 6–8). Activity increased with increasing reaction temperature from 2.83×10^6 to 2.88×10^6 and to 3.10×10^6 g_{polymer} mol_{Fe}⁻¹ h⁻¹ at 30, 40 and 50 °C respectively (Table 1: entries 1, 6 and 7). Catalyst activity, however, decreased to 2.42×10^6 g_{polymer} mol_{Fe}⁻¹ h⁻¹ at 60 °C (Table 1: entry 8). It is evident from these observations that at 60 °C the catalysts start to decompose and that optimum temperature for this catalyst is 50 °C; however, at 60 °C it appears chain transfer [19–22] or chain termination [8–10] is favoured over chain propagation. This leads to lower molecular weight polymers and some degree of branching of the poly(1-hexene) (Table 1: entries 1, 6–8). Significantly, the polydispersity indices remained narrow and

did not change with the variations in temperature, indicating that the active sites for propagation in the catalysts are not affected by increase in reaction temperature. Marques *et al.* [32] have also reported this observation where narrow polydispersity indices are observed at temperatures ranging from -1 to 25 °C.

Different monomer concentrations were also investigated by varying the monomer equivalents. Increase in both the productivity and activity were observed when the monomer equivalent was increased from 1500 to 2000 (Table 1: entries 1 and 9) with a corresponding increase in polymer molecular weight. However, catalyst activity decreased slightly when the monomer concentration was increased to 2500, an observation which is likely due to saturation of the system. The resultant polymer M_n varies from 1045 Da to 1038 Da to 1084 Da as monomer equivalents increased from 1500 to 2000 and 2500 respectively (Table 1: entries 1, 9 and 10).

2.3. Characterization of Poly(1-hexene) Using ^1H NMR Spectroscopy

The microstructure of the poly(1-hexene) obtained using pre-catalyst 1 with EtAlCl_2 as co-catalyst (Table 1: entry 1) was studied using ^1H NMR spectroscopy (Figure S1). The ^1H NMR spectra for all the poly(1-hexene) produced under different conditions were similar to the spectrum in Figure S1. The peak at 0.83 ppm in Figure S1 is assigned to the methyl branches similar to observations made by Subramanyam *et al.* for polypropylene [45]. The signal at 0.88 ppm (triplet) (Figure S1) is due to terminal methyl groups of butyl or longer chain branches. The signals at 0.75 and 0.76 ppm in Figure S1 are part of the methyl branches of the polymer similar to what has reported for polypropylene moieties in the literature [45]. The spectrum (Figure S1) also shows a peak at 1.25 ppm characteristic of long chain methylene groups, $(\text{CH}_2)_n$. This signal can arise from branches as well as from the polymer backbone. Thus the integration of the methyl and methylene peaks determined the degree of branching calculated to be between 220 and 300. We observed no terminal olefinic end groups in the NMR spectra of the polymers. This suggests that termination and/or chain transfer reactions in the polymerization takes place via transmetalation with organoaluminum species and not by β -H elimination.

Usually highly branched polyolefins are produced using nickel catalysts [46–48]. This is because nickel catalysts readily undergo metal migration through a series of β -hydride transfers. An example is Brookhart's (α -diimine)nickel(II) chloride catalyst that polymerises propylene, 1-hexene and 1-octadecene to highly branched polyolefins; some of these polymers have degree of branching as high as 297 per 1000 carbons [19–22]. To understand further the microstructure of our poly(1-hexenes), $^{13}\text{C}\{^1\text{H}\}$ NMR experiments were performed on these polymers.

2.4. Characterization of Poly(1-hexene) Using $^{13}\text{C}\{^1\text{H}\}$ NMR Spectroscopy

A typical $^{13}\text{C}\{^1\text{H}\}$ NMR spectrum of the poly(1-hexene) is shown in Figure 1 and Figures S2–S4 show other $^{13}\text{C}\{^1\text{H}\}$ NMR spectra that were used to determine the branched nature of poly(1-hexenes) obtained. Almost all the peaks in Figure 1 have been assigned according to reported nomenclature [49,50], and tabulated in Table 2. The peaks that were not assigned have been marked with asterisk. In Table 2, the first column represents the numbering of peaks in Figure 1; the second column the chemical shifts, the third column resonance integral values relative to the integral value of peak 1 and the last column the carbon branch assignments. The signal at 14.13 ppm (peak 1, Figure 1) is assigned to the methyl carbon of butyl ($^1\text{B}_4$) or longer chain branches ($^1\text{B}_n$). The signal at 19.76 ppm (peak 3) is assigned exclusively to the methyl branches and is similar to branching in polypropylene [45]. The observed multiplicity of peaks can be explained in terms of tacticity effects. Generally, the branches with methyl peaks appear in the region 14.00–17.00 ppm. It is possible that these correspond to the methyl proton signals observed in the region 0.75–0.83 ppm. Similar peaks have been observed in the poly(1-hexene) synthesised by Subramanyam *et al.* [45]. Peaks 6 (26.44–27.59 ppm, $^2\text{B}_2$ and $^\beta\text{B}_2$), 17 (33.77 ppm, $^\alpha\text{B}_2$) and 21 (39.62 ppm, brB_2) are designated to ethyl branches, while the propyl branches are observed at 14.58 ppm ($^1\text{B}_3$). Other resonances associated with propyl branches are peaks 3 ($^2\text{B}_3$), 18 ($^\alpha\text{B}_3$) and 20 (brB_3). Signals typical of butyl branches are also observed at 14.13 ppm (peak 1, $^1\text{B}_4$),

23.22–23.25 ppm (peak 5, 2B_4), 28.21 and 29.76 ppm (peaks 8 and 9, 3B_4). Longer chain branches are also present as a result of chain running. They are represented by branches with $n > 4$ whose methylene carbon is observed at 22.76 ppm (peak 4, 2B_n), 29.76 ppm (peak 10, 4B_n) and 32.45 ppm (peak 15, 3B_n).

Table 2. Chemical shifts and assignments for the numbered peaks in Figure 1.

Peak No.	Chem. Shifts (ppm)	Integral Expt.	Carbon Atom Assignment
1	14.13	1	${}^1B_4, {}^1B_n$
2	14.58	0.16	1B_3
3	19.76	0.14	1B_1
	20.09	0.05	2B_3
4	22.76	0.74	2B_n
5	23.22–23.25	0.25	2B_4
6	26.44–26.80	0.11	βB_4
	27.16	0.02	2B_2
	27.32–27.59	0.06	βB_2
7	27.9	0.1	$1,6\beta^1B_1$
8	28.21	0.06	3B_4
9	29.45	0.17	3B_4
10	29.76	0.36	${}^4B_n, 1,4\text{-}{}^4B_n$
11	30.09–30.21	0.29	γB_1
12	30.44	0.15	$1,4\text{-}\gamma B_1, 1,5\text{-}\gamma B_1$
13	30.76	0.14	br B_1
14	32.01	0.35	$1,4\text{-}\alpha^1B_n$
15	32.45	0.27	${}^3B_n, 1,4\text{-}{}^3B_n$
16	33.00	0.03	br B_1
17	33.77	0.09	4B_4
18	34.09	0.11	αB_4
	34.35	0.07	${}^4B_4, \alpha B_3$
19	35.00	0.13	$\alpha B_1, \text{br}B_3, 1,5\text{-}\alpha^1B_1$
20	37.16–37.61	0.06	$\alpha B_1, \text{br}B_3$
21	39.62	0.11	br B_2

Polyethylene type of structural units, $-(\text{CH}_2\text{-CH}_2)_n-$, are also observed with the appearance of the peak at 30.09 ppm (peak 11, γB_1). γ indicates how far the methyl group is from a branch point and this gives rise to the polyethylene type of units. A similar peak at 30.01 ppm is present in the spectra of poly(1-hexene) and EP co-polymer reported by Subramanyam *et al.* [45].

It is evident from the above ${}^{13}\text{C}\{^1\text{H}\}$ NMR data for poly(1-hexenes) obtained with pre-catalyst 1 that the polymers have micro-structures that consist of methyl, ethyl, propyl, butyl and longer branches on a polyethylene backbone. The polymers are generally atactic in structure, evident from the chemical shifts and intensities of peaks 1, 4, 9, 10, 14, 15 and 21.

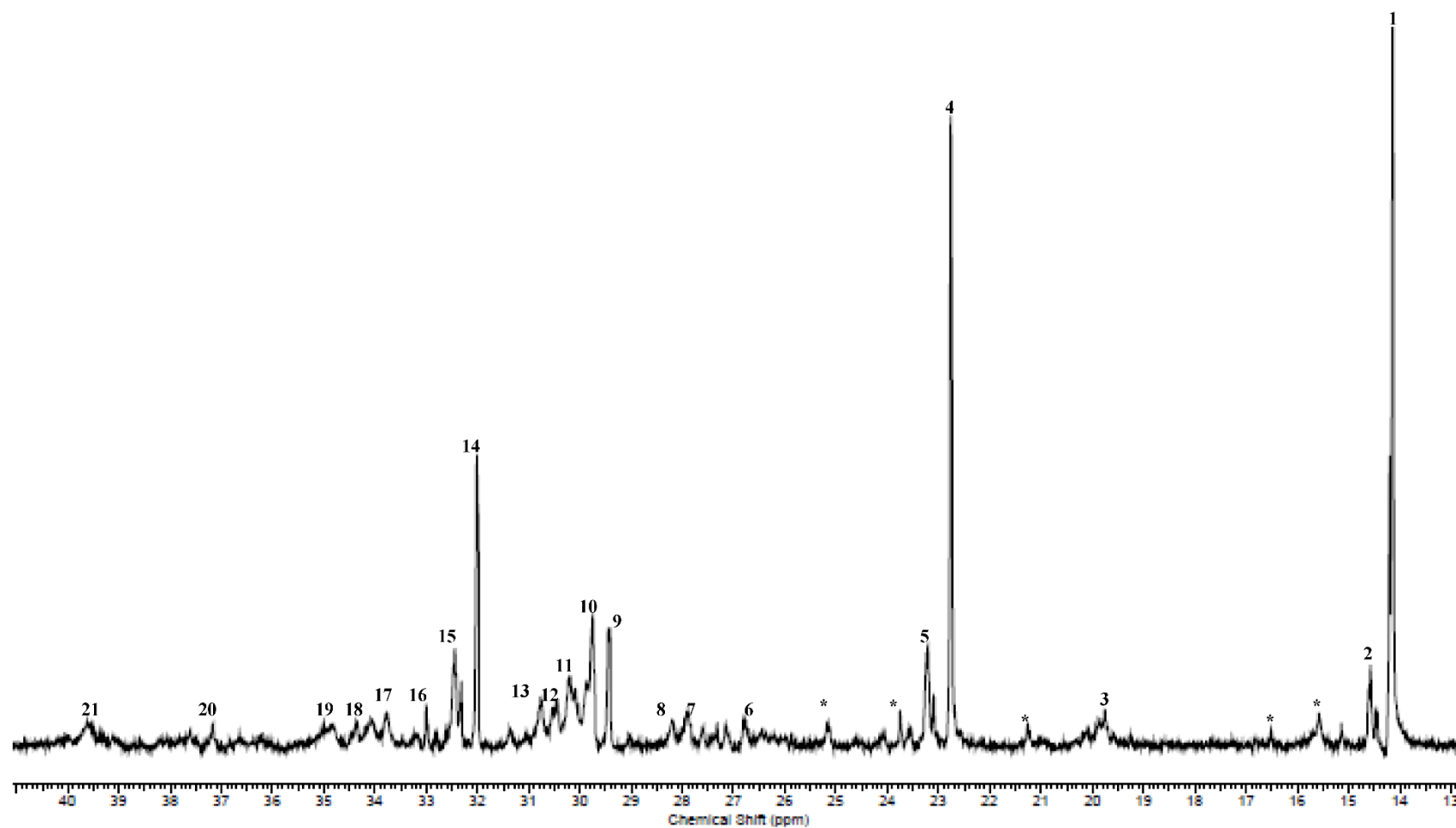


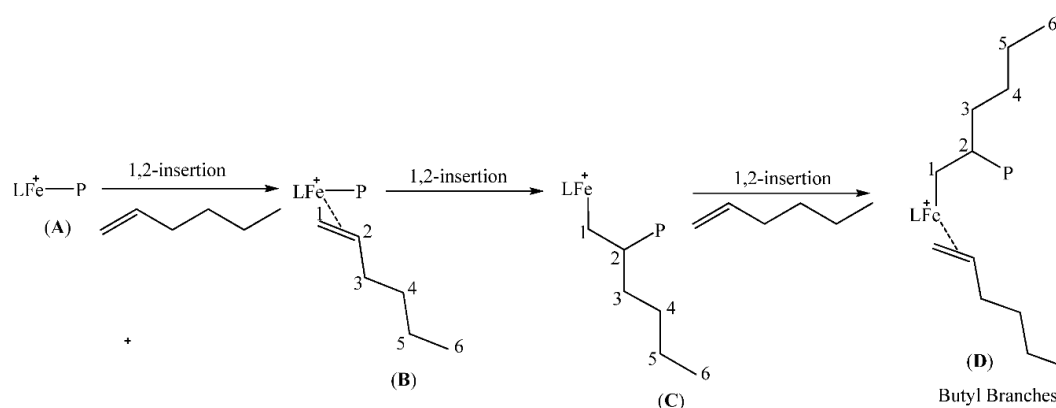
Figure 1. $^{13}\text{C}\{^1\text{H}\}$ NMR spectrum of the poly(1-hexene) obtained using (salicylaldehyde)iron(III) pre-catalyst 1 (Table 1: entry 1). The peaks marked with asterisk were not assigned.

2.5. Rationalisation of Formation of the Different Branches in the Poly(1-hexene) Microstructure

The formation of the different types of branches in our poly(1-hexene) are explained by the regiochemistry of monomer insertion; and these are typical of chain growth where 2,1-insertion of the 1-hexene monomer into the iron-polymer bond during the polymerisation process is quite high. This is the result of the ability of the metal centre to migrate along the growing polymer chain through β -hydride elimination and reinsertion steps. Schemes 1–4 which are based on reports in literature [13,31,45,51,52], are used to rationalise how the various branching occur. The percentage of each type of branch with respect to the total branching was also calculated according to literature procedure [45]. The main branches were determined to be methyl (17%), butyl (30%) and longer chains (43%) while ethyl (3%) and propyl (7%) branches were present but in small percentages compared to the total branching.

2.5.1. Butyl Branches

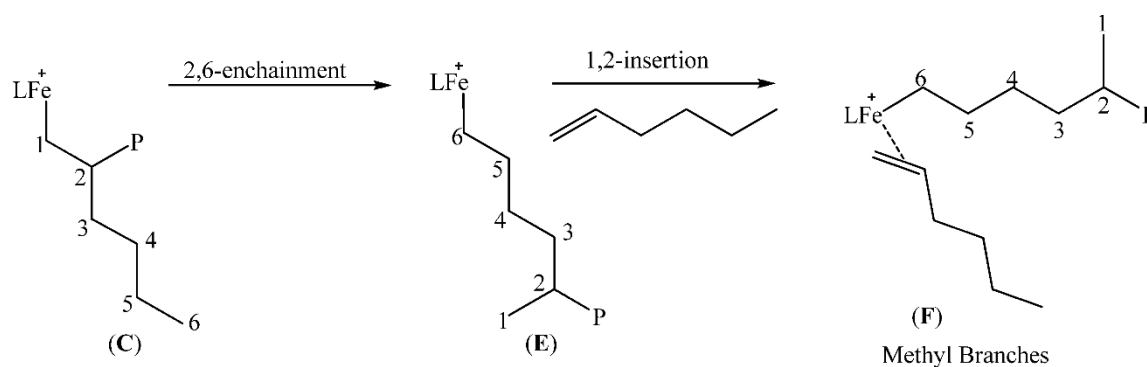
These arise from successive 1,2-insertion of 1-hexene into the iron-carbon bond A (Scheme 2) to form D.



Scheme 2. Formation of butyl branches in 1-hexene polymerization.

2.5.2. Methyl Branches

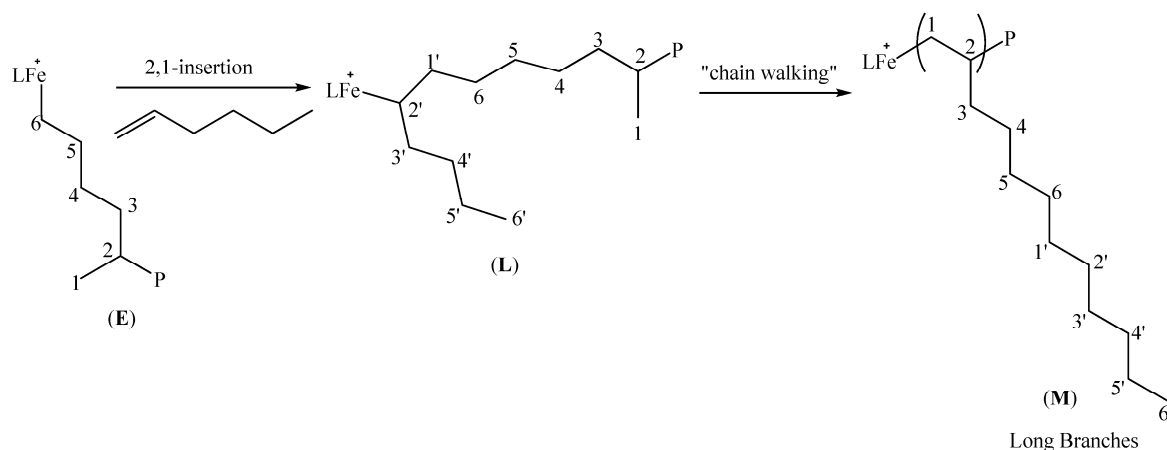
For methyl branches to be formed there is 1,2-insertion of 1-hexene to form C (Scheme 3) followed by migration of the iron metal centre by a series of β -hydride elimination till the terminal carbon (2,6-enchainment) forming E.



Scheme 3. Formation of methyl branches in 1-hexene polymerization.

2.5.3. Long Chain Branches

The dominant branches in the polymers are long chains longer than butyl. These long chain branches results from an initial 2,1-insertion of 1-hexene into the active catalyst depicted by (E) in Scheme 4 to form (L). The 2,1-insertion therefore results in the butyl branch near the Fe centre, but subsequent “chain walking” to the primary carbon gives rise to the resultant long chains in the polymer depicted in (M) (Scheme 4).



Scheme 4. Formation of long chain branches in 1-hexene polymerization.

2.6. Effect of Reaction Conditions on the Poly(1-hexene) Microstructure

The microstructure of the poly(1-hexene) obtained is likely to be affected by reaction conditions particularly reaction temperature and monomer concentration. As such the microstructure of polymers produced at a different reaction temperature and monomer concentrations were monitored by ¹³C{¹H} NMR spectroscopy. The effect of temperature on the microstructure of the poly(1-hexene) was investigated at 50 °C for 1 h with 2000 monomer equivalent. The percentage of butyl branches remained the same at 30% whereas the percentage of longer chain branches decreased from 43% to 39% at 30 and 50 °C respectively. Methyl branches on the other hand showed a significant increase from 17% (30 °C) to 20% (50 °C) which implies that the rate of 2,6-enchainment and chain walking process is increased at elevated reaction temperature. Such observation has also been reported by Azoulay *et al.* [13]. Ethyl (5%) and propyl (6%) branches were still observed but did not follow any clear trend.

Varying the monomer concentration by varying the monomer equivalent from 1500 to 2000 and to 2500 at 30 °C for 1 h did not present any clear trend either. Long chain branches were the dominant branches observed (69% (1500) to 43% (2000) to 50% (2500)). However, the amount of butyl branches increased as the monomer equivalent increased from 1500 (29%) to 2000 (30%) and to 2500 (31%). This is expected as increase in monomer concentration favours 1,2-insertion [31].

3. Experimental Section

3.1. General Materials and Instrumentations

All procedures were performed under dry Argon using standard Schlenk techniques. All solvents were of analytical grade, were dried and distilled under nitrogen prior to use. The compounds FeCl₂, 1-hexene and ethylaluminium dichloride (EtAlCl₂, 1.0 M in hexane) were purchased from Sigma-Aldrich (Johannesburg, South Africa) and used as received. The ligand, 2,4-di-*tert*-butyl-6-[(2-pyridin-2-yl-ethylimino)-methyl]-phenol (L3), [53] and the iron(III) pre-catalysts 1-5 [53], were prepared according to literature procedures. Infrared (IR) spectra were recorded on a Bruker Tensor 27 equipped with a diamond ATR. Elemental analyses were performed on a

Vario Elementar III microcube CHNS analyser at Rhodes University (South Africa). Mass spectra were recorded on a Waters API Quattro Micro spectrophotometer. The resulting polymers were characterized using GPC, ^1H and $^{13}\text{C}\{^1\text{H}\}$ NMR spectroscopy. Gel permeation chromatography (GPC) was measured on a SEC instrument which consists of a Waters 1515 isocratic HPLC pump, a Waters 717plus auto-sampler, Waters 600E system controller (run by Breeze Version 3.30 SPA) and a Waters in-line Degasser AF. A Waters 2414 differential refractometer was used at 30 °C in series with a Waters 2487 dual wavelength absorbance UV/Vis detector operating at variable wavelengths. Tetrahydrofuran (THF, HPLC grade, stabilized with 0.125% BHT) was used as eluent at flow rates of 1 mL·min⁻¹. The column oven was kept at 30 °C and the injection volume was 100 µL. Two PLgel (Polymer Laboratories) 5 µm Mixed-C (300 × 7.5 mm) columns and a pre-column (PLgel 5 µm Guard, 50 × 7.5 mm) were used. Calibration was done using narrow polystyrene standards ranging from 580 to 2 × 10⁶ g mol⁻¹. All molecular weights were reported as polystyrene equivalents. Samples for SEC were dissolved in BHT stabilized THF (2 mg mL⁻¹). Sample solutions were filtered via syringe through 0.45 µm syringe filters before subjected to analysis. The NMR spectra were recorded on a Bruker 400 MHz instrument (^1H at 400 MHz and $^{13}\text{C}\{^1\text{H}\}$ at 100 MHz) at room temperature. Chemical shifts are reported in δ (ppm) and referenced to the residual proton and (7.24 and 77.0 ppm for CDCl₃). The total number of branches per 1000 carbon atoms was calculated from the integration of the methyl and methylene signals in the ^1H NMR spectrum.

3.2. Synthesis of (2,4-Di-*tert*-butyl-6-[(2-pyridin-2-yl-ethylimino)-methyl]-phenol)Iron(III) Chloride (5)

A solution of [FeCl₂] (0.07 g, 0.57 mmol) in dichloromethane was added to a solution of 2,4-di-*tert*-butyl-6-[(2-pyridin-2-yl-ethylimino)-methyl]-phenol (**L3**) (0.19 g, 0.57 mmol) in dichloromethane. The resulting blue solution was stirred for 18 h. Analytically pure product was obtained by recrystallization from a mixture of toluene and hexane. Yield: 0.13 (50%). Anal. Calc. for C₂₂H₂₉N₂Cl₂OFe·0.5CH₂Cl₂: C, 53.33; H, 5.97; N, 5.53%. Found: C, 53.62; H, 5.97; N, 6.06%. HRMS (ESI): m/z (%) = 428.1306 (5) (M⁺-Cl), 393.1623 (10) (M⁺-2Cl), 338.2348 (10) (ligand). IR (ATR) (cm⁻¹): 1604 (s) (C=N)*v*.

3.3. General Procedure for the Polymerization of 1-Hexene

In a typical experiment, a carousel parallel reactor equipped with a magnetic stirrer was loaded with the pre-catalyst (11 µmol), higher olefin and solvent. The solution was stirred at the desired temperature for 2 min after which EtAlCl₂, the activator, was added. After the set reaction time period the reaction was quenched by adding 2 M HCl and some sampled for GC analysis. The organic phase was then separated from the aqueous phase and washed three times with water. The organic phase was dried over anhydrous MgSO₄ and the solvent evaporated to obtain the viscous oily product. The oily product was dried until a constant weight was obtained.

4. Conclusions

A new set of iron(III) pre-catalysts produce active catalysts for the polymerisation of 1-hexene with ethylaluminium dichloride (EtAlCl₂), resulting in branched poly(1-hexenes) with low molecular weights. The narrow polydispersity indices regardless of reaction condition demonstrate that these are excellent single-site late transition metal catalysts. The $^{13}\text{C}\{^1\text{H}\}$ NMR data confirm the branching in the polymers to be mainly methyl, butyl and longer chains higher than butyl; the dominant longer chain branches indicate that 2,1-insertion of monomer is favoured in the polymerisation reactions.

Acknowledgments: We acknowledge the DST-NRF Centre of Excellence in Catalysis (c*change), the National Research Foundation (NRF), South Africa and the University of Johannesburg for financial support for this project.

Author Contributions: Margaret Yankey synthesized the catalysts and performed most of the catalytic reactions, while Collins Obuah performed some of the characterisation of the polymers and interpretation of the ^{13}C NMR data; and James Darkwa conceived the project. The initial draft of the paper was by Margaret Yankey; while

the final copy and corrections made at various stages of this paper was done by the corresponding author, James Darkwa.

Conflicts of Interest: The authors declare no conflict of interest.

References

1. Morse, P.M. Demand for Synthetic Lubricants on the Rise- Greater Reliability, Stability help Synthetics gain favor over Petroleum Derivatives. *Chem. Eng. News* **1998**, *76*, 21–22. [[CrossRef](#)]
2. Brintzinger, H.H.; Fischer, D.; Miilhaupt, R.; Rieger, B.; Waymouth, R.M. Stereospecific Olefin Polymerization with Chiral Metallocene Catalysts. *Angew. Chem. Int. Ed. Engl.* **1995**, *34*, 1143–1170. [[CrossRef](#)]
3. Bochmann, M. Cationic Group 4 Metallocene Complexes and their role in Polymerisation Catalysis: The Chemistry of well-defined Ziegler Catalysts. *J. Chem. Soc., Dalton Trans.* **1996**, 255–270. [[CrossRef](#)]
4. Marks, T.J. Surface-bound Metal Hydrocarbyls. Organometallic Connections between Heterogeneous and Homogeneous Catalysis. *Acc. Chem. Res.* **1992**, *25*, 57–65. [[CrossRef](#)]
5. Chen, E.Y.-X.; Marks, T.J. Cocatalysts for Metal-Catalyzed Olefin Polymerization: Activators, Activation Processes, and Structure-Activity Relationships. *Chem. Rev.* **2000**, *100*, 1391–1434. [[CrossRef](#)] [[PubMed](#)]
6. Li, H.; Marks, T.J. Nuclearity and Cooperativity Effects in Binuclear Catalysts and Cocatalysts for Olefin Polymerization. *Proc. Natl. Acad. Sci. USA* **2006**, *103*, 15295–15302. [[CrossRef](#)] [[PubMed](#)]
7. Manz, T.A.; Phomphrai, K.; Medvedev, G.A.; Krishnamurthy, B.B.; Sharma, S.; Haq, J.; Novstrup, K.A.; Thomson, K.T.; Delgass, W.N.; Caruthers, J.M.; *et al.* Structure-Activity Correlation in Titanium Single-Site Olefin Polymerization Catalysts Containing Mixed Cyclopentadienyl/Aryloxy Ligand. *J. Am. Chem. Soc.* **2007**, *129*, 3776–3777. [[CrossRef](#)] [[PubMed](#)]
8. Ittel, S.D.; Johnson, L.K.; Brookhart, M. Late-Metal Catalysts for Ethylene Homo- and Copolymerization. *Chem. Rev.* **2000**, *100*, 1169–1204. [[CrossRef](#)] [[PubMed](#)]
9. Mecking, S. Cationic Nickel and Palladium Complexes with Bidentate Ligands for the C-C linkage of olefins. *Coord. Chem. Rev.* **2000**, *203*, 325–351. [[CrossRef](#)]
10. Gibson, V.C.; Spitzmesser, S.K. Advances in Non-metallocene Olefin Polymerization Catalysis. *Chem. Rev.* **2003**, *103*, 283–315. [[CrossRef](#)] [[PubMed](#)]
11. Johnson, L.K.; Mecking, S.; Brookhart, M. Copolymerization of Ethylene and Propylene with Functionalized Vinyl Monomers by Palladium(II) Catalysts. *J. Am. Chem. Soc.* **1996**, *118*, 267–268. [[CrossRef](#)]
12. Mecking, S.; Johnson, L.K.; Wang, L.; Brookhart, M. Mechanistic Studies of the Palladium-Catalyzed Copolymerization of Ethylene and α -Olefins with Methyl Acrylate. *J. Am. Chem. Soc.* **1998**, *120*, 888–899. [[CrossRef](#)]
13. Azoulay, J.D.; Bazan, G.C.; Galland, G.B. Microstructural Characterization of Poly(1-hexene) Obtained Using a Nickel α -Keto- β -diimine Initiator. *Macromolecules* **2010**, *43*, 2794–2800. [[CrossRef](#)]
14. Guan, Z.; Cotts, P.M.; McCord, E.F.; McLain, S.J. Chain Walking: A New Strategy to Control Polymer Topology. *Science* **1999**, *283*, 2059–2062. [[CrossRef](#)] [[PubMed](#)]
15. Younkin, T.R.; Connor, E.F.; Henderson, J.I.; Friedrich, S.K.; Grubbs, R.H.; Bansleben, D.A. Neutral, Single-Component Nickel(II) Polyolefin Catalysts That Tolerate Heteroatoms. *Science* **2000**, *287*, 460–462. [[CrossRef](#)] [[PubMed](#)]
16. Berkefeld, A.; Mecking, S. Coordination Copolymerization of Polar Vinyl Monomers $H_2C=CHX$. *Angew. Chem. Int. Ed.* **2008**, *47*, 2538–2542. [[CrossRef](#)] [[PubMed](#)]
17. Johnson, L.K.; Killian, C.M.; Brookhart, M. New Pd(II)- and Ni(II)-Based Catalysts for Polymerization of Ethylene and α -Olefins. *J. Am. Chem. Soc.* **1995**, *117*, 6414–6415. [[CrossRef](#)]
18. Leatherman, M.D.; Svejda, S.A.; Johnson, L.K.; Brookhart, M. Mechanistic Studies of Nickel(II) Alkyl Agostic Cations and Alkyl Ethylene Complexes: Investigations of Chain Propagation and Isomerization in (α -diimine)Ni(II)-Catalyzed Ethylene Polymerization. *J. Am. Chem. Soc.* **2003**, *125*, 3068–3081. [[CrossRef](#)] [[PubMed](#)]
19. Killian, C.M.; Tempel, D.J.; Johnson, L.K.; Brookhart, M. Living Polymerization of α -Olefins Using Ni^{II}- α -Diimine Catalysts. Synthesis of New Block Polymers Based on α -Olefins. *J. Am. Chem. Soc.* **1996**, *118*, 11664–11665. [[CrossRef](#)]

20. Gates, D.P.; Svejda, S.A.; Onate, E.; Killian, C.M.; Johnson, L.K.; White, P.S.; Brookhart, M. Synthesis of Branched Polyethylene Using (α -Diimine)nickel(II) Catalysts: Influence of Temperature, Ethylene Pressure, and Ligand Structure on Polymer Properties. *Macromolecules* **2000**, *33*, 2320–2334. [[CrossRef](#)]
21. Killian, C.M.; Johnson, L.K.; Brookhart, M. Preparation of Linear α -Olefins Using Cationic Nickel(II) α -Diimine Catalysts. *Organometallics* **1997**, *16*, 2005–2007. [[CrossRef](#)]
22. Svejda, S.A.; Brookhart, M. Ethylene Oligomerization and Propylene Dimerization Using Cationic (α -Diimine)nickel(II) Catalysts. *Organometallics* **1999**, *18*, 65–74. [[CrossRef](#)]
23. Meinhard, D.; Wegner, M.; Kipiani, G.; Hearley, A.; Reuter, P.; Fischer, S.; Marti, O.; Rieger, B. New Nickel(II) Diimine Complexes and the Control of Polyethylene Microstructure by Catalyst Design. *J. Am. Chem. Soc.* **2007**, *129*, 9182–9191. [[CrossRef](#)] [[PubMed](#)]
24. Yue, E.; Zhang, L.; Xing, Q.; Cao, X.-P.; Hao, X.; Redshaw, C.; Sun, W.-H. 2-(1-(2-Benzhydrylnaphthylimino)ethyl)pyridylnickel halides: Synthesis, Characterization, and Ethylene Polymerization Behaviour. *Dalton Trans.* **2014**, *43*, 423–431. [[CrossRef](#)] [[PubMed](#)]
25. Gao, R.; Sun, W.-H.; Redshaw, C. Nickel Complex Pre-catalysts in Ethylene Polymerization: New Approaches to Elastomeric Materials. *Catal. Sci. Technol.* **2013**, *3*, 1172–1179. [[CrossRef](#)]
26. Cherian, A.E.; Rose, J.M.; Lobkovsky, E.B.; Coates, G.W. A C_2 -Symmetric, Living α -Diimine Ni(II) Catalyst: Regioblock Copolymers from Propylene. *J. Am. Chem. Soc.* **2005**, *127*, 13770–13771. [[CrossRef](#)] [[PubMed](#)]
27. Rose, J.M.; Deplace, F.; Lynd, N.A.; Wang, Z.; Hotta, A.; Lobkovsky, E.B.; Kramer, E.J.; Coates, G.W. C_2 -Symmetric Ni(II) α -Diimines Featuring Cumyl-Derived Ligands: Synthesis of Improved Elastomeric Regioblock Polypropylenes. *Macromolecules* **2008**, *41*, 9548–9555. [[CrossRef](#)]
28. Rose, J.M.; Cherian, A.E.; Coates, G.W. Living Polymerization of α -Olefins with an α -Diimine Ni(II) Catalyst: Formation of Well-Defined Ethylene-Propylene Copolymers through Controlled Chain-Walking. *J. Am. Chem. Soc.* **2006**, *128*, 4186–4187. [[CrossRef](#)] [[PubMed](#)]
29. McCord, E.F.; McLain, S.J.; Nelson, L.T.J.; Arthur, S.D.; Coughlin, E.B.; Ittel, S.D.; Johnson, L.K.; Tempel, D.; Killian, C.M.; Brookhart, M. ^{13}C and 2D NMR Analysis of Propylene Polymers Made with α -Diimine Late Metal Catalysts. *Macromolecules* **2001**, *34*, 362–371. [[CrossRef](#)]
30. Galland, G.B.; da Silva, L.P.; Dias, M.L.; Crossetti, G.L.; Ziglio, C.M.; Filgueiras, C.A.L. ^{13}C NMR Determination of the Microstructure of Polypropylene obtained with the DADNi(NCS) $_2$ /methylaluminumoxane Catalyst System. *J. Polym. Sci. Part A* **2004**, *42*, 2171–2178. [[CrossRef](#)]
31. Peruch, F.; Cramail, H.; Deffieux, A. Kinetic and UV-Visible Spectroscopic Studies of Hex-1-ene Polymerization Initiated by an α -Diimine-[N,N] Nickel Dibromide/MAO Catalytic System. *Macromolecules* **1999**, *32*, 7977–7983. [[CrossRef](#)]
32. Yuan, J.-C.; Silva, L.C.; Gomes, P.T.; Valerga, P.; Campos, J.M.; Ribeiro, M.R.; Chien, J.C.W.; Marques, M.M. Living and Block Polymerization of α -Olefins using a Ni(II)- α -Diimine Catalyst Containing OSiPh $_2^t$ Bu Groups. *Polymer* **2005**, *46*, 2122–2132. [[CrossRef](#)]
33. Merna, J.; Cihlar, J.; Kucera, M.; Deffieux, A.; Cramail, H. Polymerization of Hex-1-ene Initiated by Diimine Complexes of Nickel and Palladium. *Eur. Polym. J.* **2005**, *41*, 303–312. [[CrossRef](#)]
34. Small, B.L.; Brookhart, M.; Bennett, A.M.A. Highly Active Iron and Cobalt Catalysts for the Polymerization of Ethylene. *J. Am. Chem. Soc.* **1998**, *120*, 4049–4050. [[CrossRef](#)]
35. Britovsek, G.J.P.; Gibson, V.C.; Kimberley, B.S.; Maddox, P.J.; McTavish, S.J.; Solan, G.A.; White, A.J.P.; Williams, D.J. Novel Olefin Polymerization Catalysts based on Iron and Cobalt. *Chem. Commun.* **1998**, 849–850. [[CrossRef](#)]
36. Britovsek, G.J.P.; Bruce, M.; Gibson, V.C.; Kimberley, B.S.; Maddox, P.J.; Mastroianni, S.; McTavish, S.J.; Redshaw, C.; Solan, G.A.; Stromberg, S.; *et al.* J Iron and Cobalt Ethylene Polymerization Catalysts Bearing 2,6-Bis(Imino)Pyridyl Ligands: Synthesis, Structures, and Polymerization Studies. *J. Am. Chem. Soc.* **1999**, *121*, 8728–8740. [[CrossRef](#)]
37. Britovsek, G.J.P.; Mastroianni, S.; Solan, G.A.; Baugh, S.P.D.; Redshaw, C.; Gibson, V.C.; White, A.J.P.; Williams, D.J.; Elsegood, M.R.J. Oligomerisation of Ethylene by Bis(imino)pyridyliron and -cobalt Complexes. *Chem. Eur. J.* **2000**, *6*, 2221–2231. [[CrossRef](#)]
38. Britovsek, G.J.P.; Gibson, V.C.; Kimberley, B.S.; Mastroianni, S.; Redshaw, C.; Solan, G.A.; White, A.J.P.; Williams, D.J. Bis(imino)pyridyl iron and cobalt Complexes: The Effect of Nitrogen Substituents on Ethylene Oligomerisation and Polymerisation. *Dalton Trans.* **2001**, 1639–1644. [[CrossRef](#)]

39. Britovsek, G.J.P.; Gibson, V.C.; Hoarau, O.D.; Spitzmesser, S.K.; White, A.J.P.; Williams, D.J. Iron and Cobalt Ethylene Polymerization Catalysts: Variations on the Central Donor. *Inorg. Chem.* **2003**, *42*, 3454–3465. [[CrossRef](#)] [[PubMed](#)]
40. Britovsek, G.J.P.; Gibson, V.C.; Mastroianni, S.; Oakes, D.C.H.; Redshaw, C.; Solan, G.A.; White, A.J.P.; Williams, D.J. Imine *versus* Amine Donors in Iron-Based Ethylene Polymerisation Catalysts. *Eur. J. Inorg. Chem.* **2001**, *2001*, 431–437. [[CrossRef](#)]
41. Britovsek, G.J.P.; Baugh, S.P.D.; Hoarau, O.; Gibson, V.C.; Wass, D.F.; White, A.J.P.; Williams, D.J. The Role of Bulky Substituents in the Polymerization of Ethylene Using Late Transition Metal Catalysts: A Comparative Study of Nickel and Iron Catalysts. *Inorg. Chim. Acta* **2003**, *345*, 279–291. [[CrossRef](#)]
42. Small, B.L.; Brookhart, M. Polymerization of Propylene by a New Generation of Iron Catalysts: Mechanisms of Chain Initiation, Propagation, and Termination. *Macromolecules* **1999**, *32*, 2120–2130. [[CrossRef](#)]
43. Small, B.L.; Marcucci, A.J. Iron Catalysts for the Head-to-Head Dimerization of α -Olefins and Mechanistic Implications for the Production of Linear α -Olefins. *Organometallics* **2001**, *20*, 5738–5744. [[CrossRef](#)]
44. Yankey, M.; Obuah, C.; Guzei, I.A.; Osei-Twum, E.; Hearne, G.; Darkwa, J. (Phenoxyimidazolyl-salicylaldimine)iron Complexes: Synthesis, Properties and Iron Catalysed Ethylene Reactions. *Dalton Trans.* **2014**, *43*, 13913–13923. [[CrossRef](#)] [[PubMed](#)]
45. Subramanyam, U.; Rajamohanan, P.R.; Sivaram, S. A Study of the Structure of Poly(hexene-1) Prepared by Nickel(α -diimine)/MAO Catalyst using High Resolution NMR Spectroscopy. *Polymer* **2004**, *45*, 4063–4076. [[CrossRef](#)]
46. Popeney, C.S.; Guan, Z. Effect of Ligand Electronics on the Stability and Chain Transfer Rates of Substituted Pd(II) α -Diimine Catalysts(1). *Macromolecules* **2010**, *43*, 4091–4097. [[CrossRef](#)]
47. Chen, R.; Mapolie, S.F. Catalyst Precursors for Ethylene Polymerization Based on Novel mono- and bi-Nuclear Pyridylimine-type Palladium(II) Complexes with Long Straight Chain Alkyl Substituents at the Imino Nitrogen. *J. Mol. Catal. A* **2003**, *193*, 33–40. [[CrossRef](#)]
48. Guan, Z. Control of Polymer Topology through Late-transition-metal Catalysis. *J. Polym. Sci. Part A* **2003**, *41*, 3680–3692. [[CrossRef](#)]
49. Usami, T.; Takayama, S. Fine-branching Structure in High-pressure, Low-density Polyethylenes by 50.10-MHz carbon-13 NMR Analysis. *Macromolecules* **1984**, *17*, 1756–1761. [[CrossRef](#)]
50. Galland, G.B.; de Souza, R.F.; Mauler, R.S.; Nunes, F.F. ^{13}C NMR Determination of the Composition of Linear Low-Density Polyethylene Obtained with $[\eta\text{-}3\text{-Methallyl-nickel-diiimine}]\text{PF}_6$ Complex. *Macromolecules* **1999**, *32*, 1620–1625. [[CrossRef](#)]
51. Camacho, D.H.; Guan, Z. Living Polymerization of α -Olefins at Elevated Temperatures Catalyzed by a Highly Active and Robust Cyclophane-Based Nickel Catalyst. *Macromolecules* **2005**, *38*, 2544–2546. [[CrossRef](#)]
52. Rose, J.M.; Cherian, A.E.; Lee, J.H.; Archer, L.A.; Coates, G.W.; Fetters, L.J. Rheological Behavior of Chain-Straightened Poly(α -olefin)s. *Macromolecules* **2007**, *40*, 6807–6813. [[CrossRef](#)]
53. Yankey, M.; Obuah, C.; Darkwa, J. Phenoxy-salicylaldimine-Bearing Chromium(III) Precatalysts for Ethylene Polymerization. *Macromol. Chem. Phys.* **2014**, *215*, 1767–1775. [[CrossRef](#)]

